50-mJ macro-pulses at 1064 nm from a diode-pumped picosecond laser system

A. Agnesi,[1,*] L. Carrà,[1] P. Dallocchio,[1] F. Pirzio,[1] G. Reali,[1] S. Lodo,[2] and G. Piccinno[2]

[1] *INFN and Dipartimento di Elettronica dell'Università di Pavia, Via Ferrata 1 - 27100 Pavia, Italy*
[2] *Bright Solutions Srl, Via Artigiani, 27 - 27010 Cura Carpignano (PV), Italy*
[*] *antonio.agnesi@unipv.it*

Abstract: Pulse-picking from a 100-mW cw mode-locked seeder, a hybrid master-oscillator power-amplifier (MOPA) system, based on Nd:YVO_4 and Nd:YAG amplifier modules, has been developed, delivering single-pulses of 8.6 ps at 455-MHz repetition-rate, bunched into ~1-μs trains of 50 mJ ("macro-pulses"). The output beam is linearly polarized and nearly diffraction limited up to the maximum macro-pulse repetition-rate of 50 Hz. The single-pulse peak power and the macro-pulse duration and energy are quite suitable for high-energy nonlinear optical applications such as low-threshold synchronously-pumped parametric converters in the mid infrared. The impact on the overall efficiency of saturation distortion of the macro-pulse envelope as well as of amplified spontaneous emission (ASE) is considered. The managing of the envelope distortion compensation and of the ASE suppression by means of fast saturable absorbers is reported.

OCIS codes: (140.4050) Mode-locked lasers; (140.3280) Laser amplifiers.

References and links

1. A. Agnesi, A. Del Corno, P. Di Trapani, M. Fogliani, G. C. Reali, J.-C. Diels, C. Y. Yeh, X. M. Zhao, and V. Kubecek, "Generation of extended pulse trains of minimum duration by passive negative feedback applied to solid state lasers," IEEE J. Quantum Electron. **28**(3), 710–719 (1992).
2. P. Heinz, A. Seilmeier, and A. Piskarskas, "Picosecond Nd:YLF laser-multipass amplifier source pumped by pulsed diodes for the operation of powerful OPOs," Opt. Commun. **136**(5-6), 433–436 (1997).
3. A. A. Mani, Ph. Hollander, P. A. Thiry, and A. Peremans, "All-solid-state 12 ps actively passively mode-locked pulsed Nd:YAG laser using a nonlinear mirror," Appl. Phys. Lett. **75**(20), 3066–3068 (1999).
4. A. Agnesi, G. C. Reali, V. Kubecek, S. Kumazaki, Y. Takagi, and K. Yoshihara, "β-barium borate and lithium triborate picosecond parametric oscillators pumped by a frequency-tripled passive negative-feedback mode-locked Nd:YAG laser," J. Opt. Soc. Am. B **10**(11), 2211–2217 (1993).
5. A. A. Mani, L. Dreesen, P. Hollander, C. Humbert, Y. Caudano, P. A. Thiry, and A. Peremans, "Pumping picosecond optical parametric oscillators by a pulsed Nd:YAG laser mode locked using a nonlinear mirror," Appl. Phys. Lett. **79**(13), 1945–1947 (2001).
6. I. Will, G. Koss, and I. Templin, "The upgraded photocatode laser of the TESLA Test Facility," Nucl. Instrum. Meth. A **541**(3), 467–477 (2005).
7. A. Agnesi, C. Braggio, L. Carrà, F. Pirzio, S. Lodo, G. Messineo, D. Scarpa, A. Tomaselli, G. Reali, and C. Vacchi, "Laser system generating 250-mJ bunches of 5-GHz repetition rate, 12-ps pulses," Opt. Express **16**(20), 15811–15815 (2008), http://www.opticsinfobase.org/oe/abstract.cfm?URI=oe-16-20-15811.
8. A. Agnesi, C. Braggio, G. Bressi, G. Carugno, G. Galeazzi, F. Pirzio, G. Reali, G. Ruoso, and D. Zanello, "MIR status report: an experiment for the measurement of the dynamical Casimir effect," J. Phys. A: Math. Theor. **41**(16), 164024 (2008).
9. G. Edwards, R. Logan, M. Copeland, L. Reinisch, J. Davidson, B. Johnson, R. Maciunas, M. Mendenhall, R. Ossoff, J. Tribble, J. Werkhaven, and D. O'Day, "Tissue ablation by a free-electron laser tuned to the amide II band," Nature **371**(6496), 416–419 (1994).
10. http://www.mirsurg.eu/
11. A. Agnesi, F. Pirzio, A. Tomaselli, G. Reali, and C. Braggio, "Multi-GHz tunable-repetition-rate mode-locked Nd:$GdVO_4$ laser," Opt. Express **13**(14), 5302–5307 (2005), http://www.opticsinfobase.org/oe/abstract.cfm?URI=oe-13-14-5302.
12. J. E. Bernard and A. J. Alcock, "High-efficiency diode-pumped Nd:YVO_4) slab laser," Opt. Lett. **18**(12), 968–970 (1993).
13. A. Agnesi, P. Dallocchio, L. Carrà, F. Pirzio, G. Reali, A. Tomaselli, D. Scarpa, and C. Vacchi, "210-μJ

#148862 - $15.00 USD Received 7 Jun 2011; revised 4 Jul 2011; accepted 4 Jul 2011; published 3 Oct 2011

picosecond pulses from a quasi-cw Nd:YVO_4 grazing-incidence two-stage slab amplifier package," IEEE J. Quantum Electron. **44**(10), 952–957 (2008).
14. D. Sauder, A. Minassian, and M. Damzen, "High efficiency laser operation of 2 at.% doped crystalline Nd:YAG in a bounce geometry," Opt. Express **14**(3), 1079–1085 (2006), http://www.opticsinfobase.org/oe/abstract.cfm?URI=oe-14-3-1079.
15. T. Omatsu, K. Nawata, M. Okida, and K. Furuki, "MW ps pulse generation at sub-MHz repetition rates from a phase conjugate Nd:YVO_4) bounce amplifier," Opt. Express **15**(15), 9123–9128 (2007), http://www.opticsinfobase.org/oe/abstract.cfm?URI=oe-15-15-9123.
16. L. M. Frantz and J. S. Nodvik, "Theory of pulse propagation in a laser amplifier," J. Appl. Phys. **34**(8), 2346–2349 (1963).
17. D. N. Schimpf, C. Ruchert, D. Nodop, J. Limpert, A. Tünnermann, and F. Salin, "Compensation of pulse-distortion in saturated laser amplifiers," Opt. Express **16**(22), 17637–17646 (2008), http://www.opticsinfobase.org/oe/abstract.cfm?URI=oe-16-22-17637.
18. *www.batop.de*, BATOP GmbH, Jena (Germany).
19. R. Grange, M. Haiml, R. Paschotta, G. J. Spühler, L. Krainer, M. Golling, O. Ostinelli, and U. Keller, "New regime of inverse saturable absorption for self-stabilizing passively mode-locked lasers," Appl. Phys. B **80**, 151–158 (2005).
20. A. A. Shilov, G. A. Pasmanik, O. V. Kulagin, and K. Deki, "High-peak-power diode-pumped Nd:YAG laser with a Brillouin phase-conjugation--pulse-compression mirror," Opt. Lett. **26**(20), 1565–1567 (2001).
21. P. Peuser, W. Platz, P. Zeller, T. Brand, M. Haag, and B. Köhler, "High-power, longitudinally fiber-pumped, passively Q-switched Nd:YAG oscillator-amplifier," Opt. Lett. **31**(13), 1991–1993 (2006).
22. C. Wandt, S. Klingebiel, M. Siebold, Z. Major, J. Hein, F. Krausz, and S. Karsch, "Generation of 220 mJ nanosecond pulses at a 10 Hz repetition rate with excellent beam quality in a diode-pumped Yb:YAG MOPA system," Opt. Lett. **33**(10), 1111–1113 (2008).

1. Introduction

Solid-state laser systems generating trains of hundreds of picosecond pulses at high energy levels in the near infrared (~1 mJ and higher) with reliable Nd^{3+}:host technology [1–3] have been proved to be very effective excitation sources for synchronously-pumped optical parametric oscillators (SPOPOs) ranging from the UV [4] to the mid- and far-infrared [5]. Other applications of laser systems with such a pulse format have been demonstrated as photocathode injectors [6], or even more peculiar ones such as for high-frequency excitation of a longitudinally-oscillating "plasma mirror" in a microwave cavity for the induction and detection of the long-sought dynamic Casimir effect [7,8].

Compared to our previous work reported in Ref [7], where the high-energy amplifiers were flashlamp-pumped Nd:YAG rods, here we present the first, to our knowledge, all-diode-pumped MOPA system delivering picosecond pulse trains of up to few microsecond duration, with energy as high as 50 mJ at 1064 nm. The single-pulse width was 8.6 ps at a repetition-rate of 455 MHz. The seeder was a compact 100-mW cw mode-locked Nd:YVO_4 oscillator. A hybrid combination of amplifiers based on high-gain Nd:YVO_4 and high-storage Nd:YAG slabs have been employed.

Resonant saturable absorber mirrors (RSAMs) have also been employed for suppression of self-oscillation and ASE background in the high-gain amplifier chain. Compared to previous high-energy passively mode-locked oscillators stabilized through negative feedback by self-defocussing from a GaAs plate [1,3], this architecture shows greater flexibility as the macro-pulse format is managed through fast modulation of the cw mode-locked seeder output. Indeed, macro-pulse distortions occurring in the saturated amplifiers can be compensated by shaping the appropriate seed envelope with the acousto-optic modulator (AOM).

This laser system was designed and built as a pump source for ~6.5−μm SPOPOs with a pulse format closely matching that of a free-electron laser used to carry out preliminary studies of minimally invasive surgery at that wavelength [9], as a part of the EU project MIRSURG [10]. The relatively high single-pulse repetition rate is very appealing for the realization of robust, compact and portable SPOPOs for practical uses.

#148862 - $15.00 USD Received 7 Jun 2011; revised 4 Jul 2011; accepted 4 Jul 2011; published 3 Oct 2011

2. Laser system and experimental results

The laser system is shown schematically in Fig. 1. The seeder is a 455-MHz diode-pumped Nd:YVO_4 oscillator, mode-locked with a semiconductor saturable absorber mirror. All cavity mirrors are high-reflectivity, and the 2% output coupling is taken through the reflection from the quasi-Brewster-cut face of the Nd:YVO_4 crystal as in Ref [11]. The 100-mW output beam with 5.4-ps pulses (fwhm) is then sampled by a fast AOM (AA Opto-Electronic MT200-A0.2-1064), yielding a macro-pulse envelope length ≥ 100 ns, which can readily be shaped in order to compensate for amplifiers saturation and deliver a sufficiently flat-top final output envelope. Envelope durations in the range 500-1000 ns were chosen, according to the target application requirements.

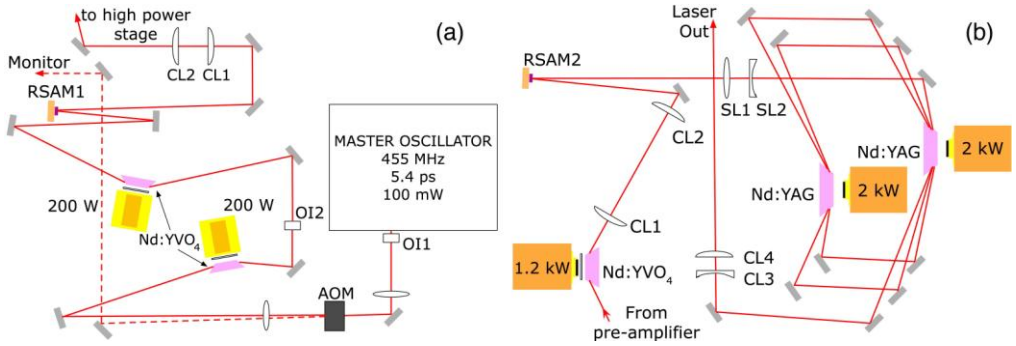

Fig. 1. Amplifier setup. Low-power section (a) and high-power modules (b). OIs: Faraday opto-isolators; CLs: cylindrical lenses; SLs: spherical lenses.

A first high-gain amplifier module uses two 4 × 2 × 12 mm^3 slabs of 1%-doped Nd:YVO_4, in a grazing-incidence configuration [12–15], each pumped at 808 nm by a 200-W linear diode array. The macro-pulse energy increases from 45 nJ to 1.2 mJ. A high-energy pre-amplifier module employing a 1.2-kW stacked diode array pumping a larger (4 × 4 × 20 mm^3) 1% Nd:YVO_4 slab at 808 nm increases further the energy to 6 mJ. Two RSAM devices, sandwiching this pre-amplifier, reduce both ASE and the tendency to self-oscillation.

Owing to the very high total gain, we chose to operate the amplifiers not at full power, thus trading off stability and efficiency. The vanadate amplifiers are pumped with polarization parallel to *c*-axis and 100-μs pulses, matching the fluorescence lifetime of the laser crystal.

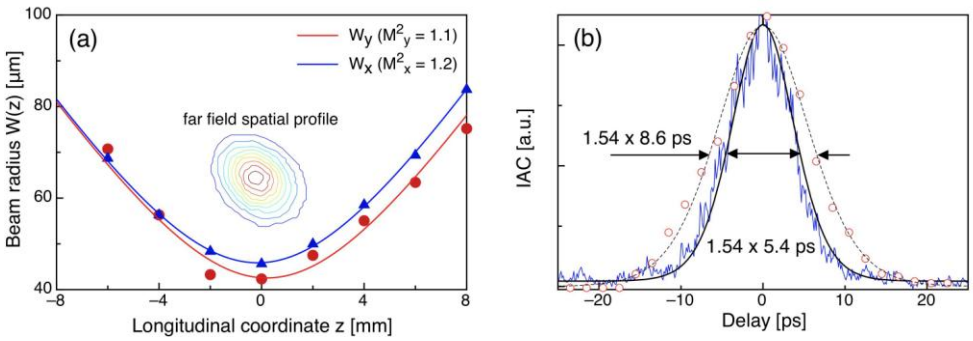

Fig. 2. Beam quality measurement near the focus of a spherical lens (a). Second-harmonic intensity autocorrelations (oscillator: 5.4 ps fwhm, amplifier: 8.6 ps, *sech*^{2} deconvolution) (b).

The high-energy amplifier section is also operated in a bounce multipass scheme within two 6 × 6 × 30 mm^3 1% Nd:YAG modules (three and two passes in each module, respectively), each pumped by a 2-kW stacked diode array at 810 nm, rising the energy up to 50 mJ in a nearly diffraction limited (Fig. 2) and polarized output beam, at repetition rates ≤

#148862 - $15.00 USD Received 7 Jun 2011; revised 4 Jul 2011; accepted 4 Jul 2011; published 3 Oct 2011

50 Hz limited by stacks ratings. The pump pulses in this last stage are 200-μs long, to take advantage of the fluorescence time of Nd:YAG. The multipass helped increase the effective beam area and the energy extraction. Output single-pulse duration is increased to 8.6 ps owing to gain narrowing in the amplifiers, like in Ref [7]. Macropulse energy fluctuations were within +/–3% over one hour around the average value.

3. Performance analysis of the amplifier modules and distortion compensation

For each amplifier module, both the small-signal gain G_0 and the saturation energy E_{sat} can be inferred by comparison of the input and output macro-pulse waveforms and their energy. Indeed, Frantz-Nodvik equations [16] yield the output envelope power $P_o(t)$ at time t for the correspondent input power $P_i(t)$:

$$P_o(t) = \frac{P_i(t)}{1-(1-1/G_0)\exp[-E_i(t)/E_{sat}]} \tag{1}$$

where

$$E_i(t) = \int_{-\infty}^{t} P_i(t')dt' \tag{2}$$

Therefore, running a simple best-fit routine (a Matlab™ script of a few lines, in our case), given the input (E_i) and output (E_o) energy as well as the respective waveforms stored by a digital oscilloscope, one can readily extract both G_0 and E_{sat} (see for example Fig. 3).

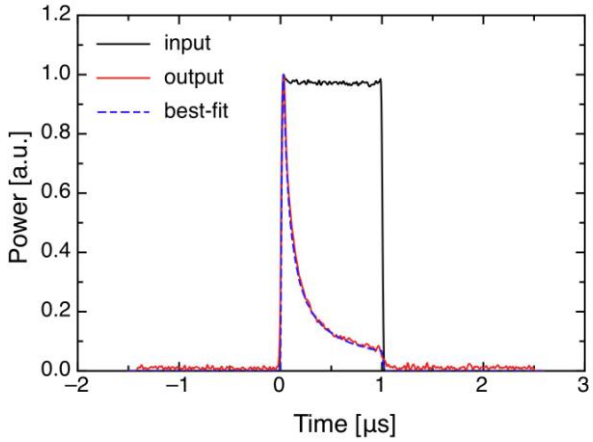

Fig. 3. Example of best-fit allowing determination of G_0, E_{sat} for the first high-gain module.

Table 1. Result of the characterization of the amplifier modules.

amplifier		G_0 [dB]	E_{sat} [mJ]	Beam spot size
stage	Pump module diode array(s)			
I	2 x 200 W	49.0	0.60	circular, w = 0.5 mm
II	1.2 kW	17.2	1.51	elliptic, w_x = 0.6 and w_y = 1.3 mm
III	2 x 2 kW	22.6	19.0	circular, w = 1.0 mm

The "error" parameter for the optimization function is defined as the rms waveform difference normalized to the area. The input waveform does not need to be flat-topped actually, since the software can easily manage any arbitrary envelope profile. The most natural choice for the sampling time interval is the oscillator round-trip time of 2.2 ns. With such a method we could fully characterize each amplifier module, as summarized in Table 1.

#148862 - $15.00 USD Received 7 Jun 2011; revised 4 Jul 2011; accepted 4 Jul 2011; published 3 Oct 2011

Schimpf et al. [17] managed to find the inverse form of Eq. (1) in order to determine the input waveform required to yield a given output waveform, once the amplifier parameters G_0 and E_{sat} are known. They remarked that a straightforward derivative of the relation between input and output fluences yields the answer. This provides a means for achieving an arbitrary output waveform simply modulating the input envelope appropriately.

In a multi-stage system, like that described in this work, according to the approach outlined in Ref [17]. one should start from the last stage and trace the amplifier chain backward to determine the input waveform for a given output energy. In our particular situation, the output energy is not generally known in advance; instead, the maximum input power is known and it can be modulated with an appropriate step-wise function $0 < f_m \leq 1$. Furthermore, the presence of additional nonlinear elements such as the RSAMs increases the overall complexity, hence a numerical best-fit approach, also for determining the f_m values required for a flat-topped output beam, is preferred. In this case, the functional "error" to be minimized was the rms deviation from the target flat-top output shape divided by the output energy. This ensures that both a flat-topped waveform and the highest output energy result from a suitable f_m modulation function.

The ripple of the simulated output waveform in Fig. 4 (6.6% standard deviation) is due to the microprocessor sampling time of 25 ns and to the amplifier saturation occurring on such short interval owing to the very high gain. A microprocessor, feeding f_m to the AOM driver at three times faster speed rate, would reduce such ripple to 2.3%. However, the waveform f_m is eventually slightly adjusted in few iterations, observing its influence on the laser output envelope, in order to generate a sufficiently flat-top macro-pulse (Fig. 4). Beam cross-section changes during saturation, as well as other effects not accounted for by our model, are responsible for prediction errors, especially when the high-gain amplifier chain is tested.

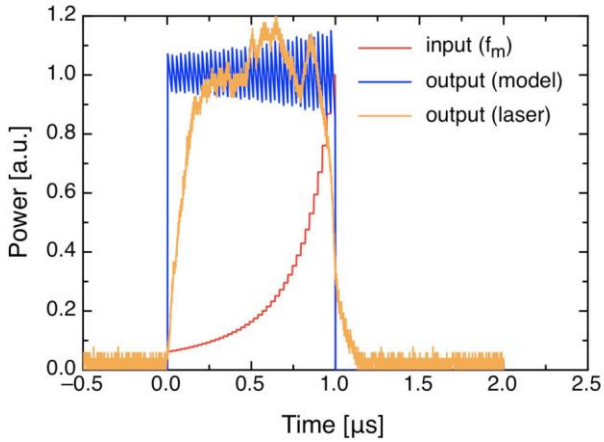

Fig. 4. Left: Waveform shaping for the overall system (numerical and measured waveforms).

4. Noise suppression with RSAMs

According to the manufacturer's specifications and the device characterization report [18], the physical model of the energy-dependent reflectivity of the RSAM, including two-photon absorption (TPA) is that proposed in Ref [19]:

$$R(F_p) = 1 - A_{ns} - \frac{\Delta R\,(1 - e^{-F_p / F_{sn}})}{F_p / F_{sn}} - \frac{F_p}{I_{TPA}\,\tau} \qquad (3)$$

where F_p is the single-pulse fluence and τ its pulse-width, A_{ns} = 0.18 the non-saturable loss, ΔR = 0.81 the saturable loss, F_{sn} = 105 μJ/cm^2 the saturation fluence of the RSAM. I_{TPA} = 17

#148862 - $15.00 USD Received 7 Jun 2011; revised 4 Jul 2011; accepted 4 Jul 2011; published 3 Oct 2011

GW/cm^2 is an "intensity" parameter corresponding to strong loss increase due to TPA: such effect quickly becomes relevant for ultrashort pulses below 1-ps duration, whereas in the 10-ps regime the RSAM should allow nearly 80% saturated reflectivity.

The spot radius on RSAM1 was 0.6 mm, and 1.3 mm on RSAM2 in order to achieve effective saturation while preventing optical damage.

In our experiments we measured at best $R \approx 40\%$ for each RSAM (integrated on the macro-pulse envelope), which necessarily is not uniform in the intermediate stages: as a matter of fact, this was the main contribution to the overall efficiency reduction.

Although we used the RSAM functional model expressed by Eq. (3) according to the data specified by the manufacturer, we remark that also in this case a best-fit routine can be run to infer the device parameters from a comparison among incident and reflected waveforms.

5. Discussion and conclusions

Considering the actual driving currents, the total input energy for the laser amplifiers was 0.896 J (170 W × 2 × 0.1 ms + 1020 W × 0.1 ms + 1900 W × 2 × 0.2 ms). Therefore, the overall optical-to-optical efficiency of the system was 50 mJ / 896 mJ = 5.6%. High-energy diode-pumped neodymium-doped multipass laser amplifiers were reported previously with slightly higher efficiency, from ≈8% [20,21] to up ≈10% for an Yb:YAG system [22]. However, we note that this particular realization was subject to special constraints not present in more ordinary situations such as the amplification of nanosecond pulses [20–22]:

- the seed energy is necessarily low, to guarantee superior operational reliability and compactness for the master oscillator, thus requiring very high total gain;
- the compactness of the overall system configured for table-top operation makes it susceptible to self-oscillation since long-focal spatial filters cannot be employed and vacuum-sealed short-focal filters were not a possible option: this forced us to choose RSAMs that unfortunately pay a significant penalty in energy reflectance;
- the requested flat-top macro-pulse output envelope also determines some energy reduction, because the seed energy is used partially (≈25%) owing to the modulation function f_m.

In order to make an estimate of the theoretical efficiency that would be available without the RSAMs and the waveform shaping, we ran the simplest Frantz-Nodvik model with a flat-top input macro-pulse (full energy) with the parameters listed in Tab. 1. A total energy of 81 mJ results, decreasing to 76 mJ due to waveform compensation for flat-topped output waveform. The inclusion of RSAMs decreases further the energy to 48 mJ, in fair agreement with our experimental measurements. Thus the maximum possible optical-to-optical efficiency for the amplifier setup would be ≈9%, assuming a single short seed pulse with the same energy of 45 nJ and virtually lossless ASE-stopping spatial filters.

In conclusion we have reported on what we believe to be the first high-energy all-diode-pumped picosecond laser system delivering 50 mJ at 1064 nm with 1-μs macro-pulse and 230 single-pulses (8.6-ps fwhm). The macro-pulse duration can be readily tuned in the range ~100 ns – few μs, and the waveform can be shaped with the programmable AOM. This laser system was designed originally as a pump source for SPOPOs in the mid-infrared for surgical applications, as a compact alternative to free-electron lasers, but it can be exploited for other interesting uses as well, that benefit from its particular pulse format.

Acknowledgements

This research received funding from the European Community's Seventh Framework Programme FP7/2007-2011 under grant agreement n° 224042 (MIRSURG project [10]). We thank S. Chaitanya Kumar for his help with autocorrelation measurements.